

mental errors. This must, of course, be so for the interaction of two like particles at nonrelativistic energies and represents an excellent check on the internal consistency of the data.

The general behavior of the Legendre coefficients illustrates the importance of higher angular momenta with increasing energy. We have found it necessary to employ Legendre coefficients up to  $a_{12}$ , which does not imply an unreasonable value of angular momentum at 14 Mev.

Although the present work establishes the differential cross sections with respect to energy and angle with rather good precision over most of the angular region, additional information is required to complete the experimental picture. Thus, neutron measurements are required to extend the  $\text{He}^3$  branch measurements to  $0^\circ$ . Moreover, the polarization of the reaction products should be determined. Theoretical calculations on the subject reactions are presently in progress at this laboratory.

## Neutron Emission Probabilities from the Interaction of 14-Mev Neutrons with Be, Ta, and Bi†

LOUIS ROSEN AND LEONA STEWART

Los Alamos Scientific Laboratory, University of California, Los Alamos, New Mexico

(Received April 17, 1957)

The spatial and spectral distributions of the neutrons from 14-Mev neutron interactions with Ta and Bi have been obtained by using nuclear emulsion detectors in conjunction with a neutron collimator. These results indicate that roughly 85 to 90% of the interactions proceed via compound-nucleus formation while approximately 10 to 15% proceed by "direct" interactions. The space-integrated neutron spectrum has been obtained for Be by means of a sphere experiment. Cross sections for neutron emission, nonelastic scattering,  $(n,n')$ , and  $(n,2n)$  are derived for all three elements.

### I. INTRODUCTION

THE spatial and spectral distributions of the neutrons emitted when heavy elements are irradiated by fast neutrons yield information concerning the basic mechanism of such interactions. Specifically, these data shed light on (a) the type of interaction processes involved: for example, the relative probability of compound-nucleus formation *versus* interactions involving a small number of nucleons, (b) level density of the residual nucleus, and (c) the applicability of various nuclear models.

Previous experiments have yielded data which are not in complete harmony with any one of the currently popular nuclear models. The low-energy neutron distribution has the shape expected from the statistical

model of the nucleus, even at very high incident energies, but the high-energy tail contains too many neutrons. Though the "temperatures" and level densities are approximately those predicted by the statistical model, these quantities exhibit a disconcerting invariance with regard to mass number and excitation energy of the residual nucleus. It would almost appear as though the "temperature" of the residual nucleus cannot exceed several Mev regardless of the incident particle energy. Whether this be due to a "melting" effect,<sup>1</sup> to the emission of particles in times shorter than required for exchange of energy between the incident nucleus and the nucleons in the target nucleus, or to other effects, is at present far from clear. Recent results on  $(p,xn)$  reactions<sup>2</sup> for 12- to 85-Mev protons on Pb and Bi indicate that the compound-nucleus process is dominant at least up to 30 Mev. However,  $(p,xn)$  experiments<sup>3</sup> and  $(n,n')$  experiments<sup>4</sup> yield nuclear temperatures ( $\tau$ ) which appear to be a factor of 2 lower than those derived from  $(\alpha,n)$  and  $(\alpha,2n)$  experiments.<sup>5</sup>

Previous to the initiation of the present experiments on Ta and Bi, essentially all nonelastic neutron measurements had been concerned with the total cross sections for this process or with space-integrated neutron spectra. The present measurements give, in addition,

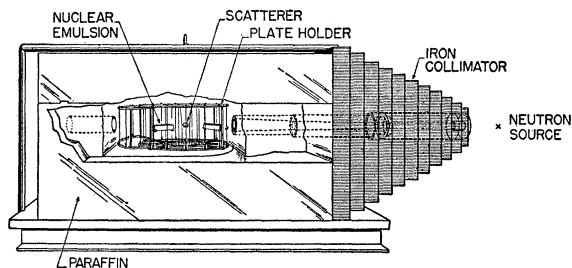


FIG. 1. Experimental arrangement for measuring angular distributions.

† This work was performed under the auspices of the U. S. Atomic Energy Commission.

<sup>1</sup> L. E. H. Trainor and W. R. Dixon, *Can. J. Phys.* **34**, 229 (1956).

<sup>2</sup> R. E. Bell and H. M. Skarsgard, *Can. J. Phys.* **34**, 745 (1956).

<sup>3</sup> P. C. Gugelot, *Phys. Rev.* **81**, 51 (1951).

<sup>4</sup> E. R. Graves and L. Rosen, *Phys. Rev.* **89**, 343 (1953).

<sup>5</sup> H. L. Bradt and D. J. Tendam, *Phys. Rev.* **72**, 1117 (1947).

the spatial distribution of the emitted neutrons which, it was hoped, would help distinguish between "optical model" processes, which involve a maximum of coherence in the reaction systematics and "statistical model" processes, which involve total incoherence.

Although the interaction of 14-Mev neutrons on a light element, such as Be, can hardly be expected to yield information on the applicability of the statistical model of the compound nucleus, it has the interesting features that Be contains no bound levels and the binding energy of the last neutron in Be<sup>9</sup> is quite small, only 1.66 Mev. A large ( $n,2n$ ) cross section is therefore to be expected.

## II. EXPERIMENTAL DETAILS

The present experiments on Ta and Bi were made possible by the use of a large neutron collimator of a type initially developed for observing neutron spectra from nuclear detonations<sup>6</sup> and since successfully employed on a number of experiments involving 14-Mev neutrons.<sup>7</sup> This collimator is made of iron backed by paraffin. Iron was chosen on the basis of the large value of the product of its nonelastic cross section and nuclear density and the fact that the nonelastic spectrum of emitted neutrons is much degraded. Even so, paraffin backing must be added to achieve further degradation in order to take data down to 0.5 Mev.

The experimental arrangement is shown schematically in Fig. 1. The source of neutrons was the 200-kev Cockcroft-Walton accelerator (since dismantled and replaced by a 500-kev machine) using the T( $d,n$ )He<sup>4</sup> reaction.

The cylindrical scatterer (3.18 cm by 3.18 cm) was positioned with its axis coinciding with the collimator axis, thus making optimum use of the incident neutron flux. The detectors were 1- by 3-inch 200- $\mu$  C2 emulsions, situated on a circle, whose long plate axes passed through the center of the scatterer. The scatterer-detector geometry and selection criteria afford a maximum angular spread of  $\pm 8^\circ$  and a maximum energy spread of  $\pm 7\%$ . Since the long axes of the detectors and the collimator axis were in a plane which was nearly perpendicular to the deuteron beam direction, any effect which might conceivably arise from the production of polarized neutrons in the  $d$ -T reaction was avoided. The details of plate-processing and analysis are given in previous publications.<sup>8,9</sup>

Figure 2 shows the observed and calculated beam profile at various positions behind the collimator. The calculated profile assumes perfect collimation. The spectral purity of the neutron beam was obtained by

exposing an emulsion at the position of the scatterer. After making corrections for ( $n$ , charged particle) reactions in the emulsion constituents, the resulting distribution enables one to correct for degraded neutrons scattered by the scatterer. This correction is  $\sim 3\%$ .

The Be data were taken with nuclear emulsions placed approximately 54 cm from the 14-Mev neutron source, which was surrounded by a spherical shell of wall thickness  $0.221 \times 10^{24}$  atoms/cm<sup>2</sup>. This method of evaluating cross sections for neutron emission has been previously discussed.<sup>4</sup>

The cross section with respect to energy and angle for the emission of neutrons from Ta and Bi was determined as follows: let  $F_0$  denote the neutron flux [determined by counting the alpha particles from the T( $d,n$ )He<sup>4</sup> reaction] incident on the front face of a cylindrical scatterer of face area  $A$  and length  $l$  containing  $n_0$  nuclei per cm<sup>3</sup> and  $\sigma_{tr}$  the transport cross section at 14 Mev for the element under investigation; then the primary neutron flux averaged over the scatterer is given by

$$\bar{F}_n = \frac{F_0}{l} \int_0^l e^{-\sigma_{tr} n_0 t} dt = F_0 \left( \frac{1 - e^{-\sigma_{tr} n_0 l}}{\sigma_{tr} n_0 l} \right). \quad (1)$$

If now  $F_n(E, \theta) dE$  represents the number of neutrons of energy  $E$  to  $E+dE$  emitted into  $1/R^2$  steradians at a distance  $R$  from the center of the target, the differential cross section for the emission of neutrons of energy  $E$  and angle  $\theta$  is obtained from

$$\sigma_e(E, \theta) = \frac{F_n(E, \theta) R^2}{n_0 l \bar{F}_n A}. \quad (2)$$

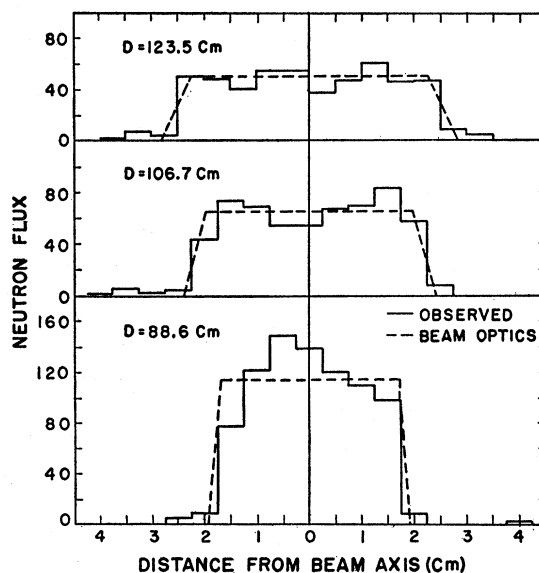


Fig. 2. Observed and calculated beam profile at various positions behind the collimator.  $D$  is the distance from source to detector.

<sup>6</sup> This type of collimator was developed in 1950 by Louis Rosen in collaboration with J. C. Allred and D. D. Phillips.

<sup>7</sup> Allred, Armstrong, and Rosen, Phys. Rev. **91**, 90 (1953).

<sup>8</sup> L. Rosen, Nucleonics **11**, No. 7, 32 (1953), and No. 8, 38 (1953).

<sup>9</sup> L. Rosen, *Proceedings of the International Conference on the Peaceful Uses of Atomic Energy, Geneva, 1955* (United Nations, New York, 1956), Vol. 4, p. 97.

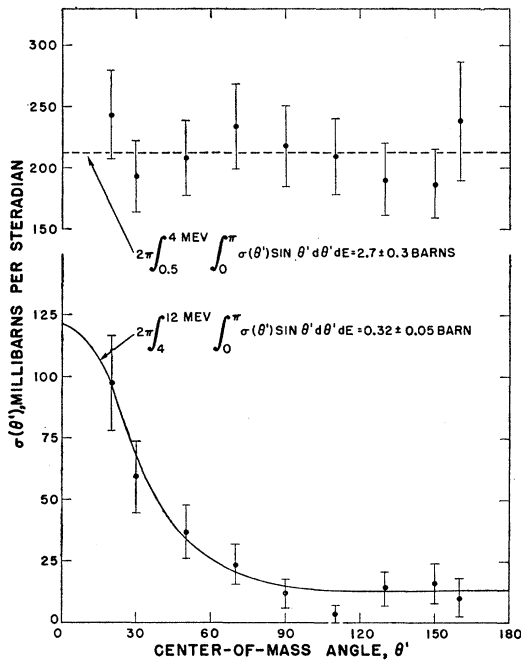


FIG. 3. Spatial distributions of the nonelastic neutrons from 14-Mev neutrons on Ta.

Finally, the flux at the detector is calculated from

$$F_n(E, \theta) dE = \frac{4\pi N(E, \theta) dE}{\sigma_{n-p}(E) 4 \langle \cos \gamma \rangle_{Av} n_p V_e \Theta P(r) A_t(E)}, \quad (3)$$

where  $N(E, \theta) dE$  = number of proton recoils between  $E$  and  $E + dE$  at angle  $\theta$ ,  $\sigma_{n-p}(E)$  = total  $n-p$  cross section at energy  $E$ ,  $\langle \cos \gamma \rangle_{Av}$  = average value of cosine of proton scattering angle,  $n_p$  = hydrogen density in emulsion,  $V_e$  = emulsion volume analyzed,  $\Theta$  = solid angle of acceptance of proton recoils,  $P(r)$  = probability that a track of range  $r$  will end within the emulsion layer, and  $A_t(E)$  = attenuation correction for neutrons in the emulsion.

### III. CORRECTIONS

Since the incident neutrons at the scatterer were not completely monoenergetic, a small correction was necessary for those degraded neutrons in the primary beam which scattered into the detectors. Only elastic scattering need be considered for these degraded neutrons. The correction was calculated on the basis of the measured spectrum at the position of the scatterer and the differential elastic scattering cross sections at the appropriate energies.<sup>10</sup>

A second correction was applied for spurious tracks from  $(n, \text{charged particle})$  reactions in the emulsion, since these cannot, in general, be distinguished from proton recoils. Since only the high-energy elastically

<sup>10</sup> D. J. Hughes and R. S. Carter, Brookhaven National Laboratory Report BNL-400, 1956 (unpublished).

scattered neutrons produce  $(n, \text{charged particle})$  reactions, the indicated correction was applied in proportion to the elastic component at each scattering angle.

Still a third correction was necessary for multiple scattering in the target. E. D. Cashwell and C. J. Everett of this Laboratory set up a Monte Carlo calculation on the MANIAC using the known cross sections for elastic and nonelastic scattering for neutrons between 0.5 and 14 Mev. The following assumptions were made:

(1) The energy distribution of the nonelastic neutrons is Maxwellian with  $\tau \sim (\text{excitation energy})^{1/2}$ .  $\tau$  values from sphere experiments at 14 Mev are adequate as a first approximation.

(2) Third and higher order collisions in the scatterer are negligible.

(3) Neutron emission always precludes  $\gamma$  emission where the former is energetically possible.

These calculations were performed with a sampling of approximately 50 000 neutrons, the first collision being forced in the usual manner. Energy distributions of the emitted neutrons which suffered either one or two collisions were compiled as a function of angle. Then, having made identical assumptions, one could calculate as a function of angle the spectrum of the neutrons which had only one collision in the target. The ratio of the number of neutrons having suffered one collision to the number having suffered one or more collisions gave

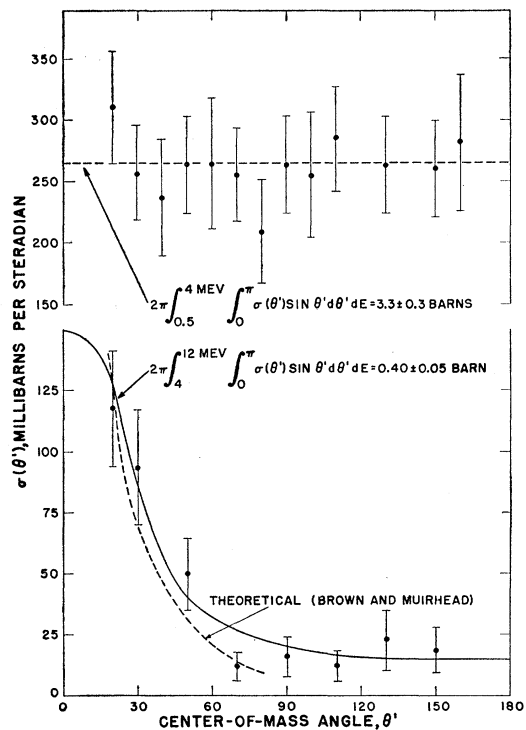


FIG. 4. Spatial distributions of the nonelastic neutrons from 14-Mev neutrons on Bi.

the correction applied to the data at any given energy and angle.

A final correction was made for the attenuation of the neutrons in the detector, as previously outlined.<sup>8</sup>

The above corrections varied from zero to 15% but they did not produce qualitative changes in the results. No corrections were made for the finite angular and energy resolution presented by the target-detector geometry.

#### IV. RESULTS

Figures 3 and 4 display the spatial distributions of the nonelastic neutrons from Ta and Bi, respectively. The space-integrated energy distributions are given in Figs. 5 and 6. The indicated uncertainties are standard deviations arrived at by a rms combination of the estimated errors in each of the quantities entering Eq. (2). (See reference 8 for a detailed discussion of these errors.) Figure 7 illustrates the degree to which the low-energy distributions from Ta and Bi may be represented by the statistical model relation:

$$F_n(E)dE = Ee^{-E/\tau}dE, \quad (4)$$

after taking account of "second" neutron emission.

The method outlined by Lang and Le Couteur<sup>11</sup> was used to obtain a temperature, for Ta and Bi, corresponding to the evaporation of the first neutron from the compound nucleus. If one assumes that two neutrons are emitted in succession and that the temperature falls as the square root of the excitation energy, the neutron

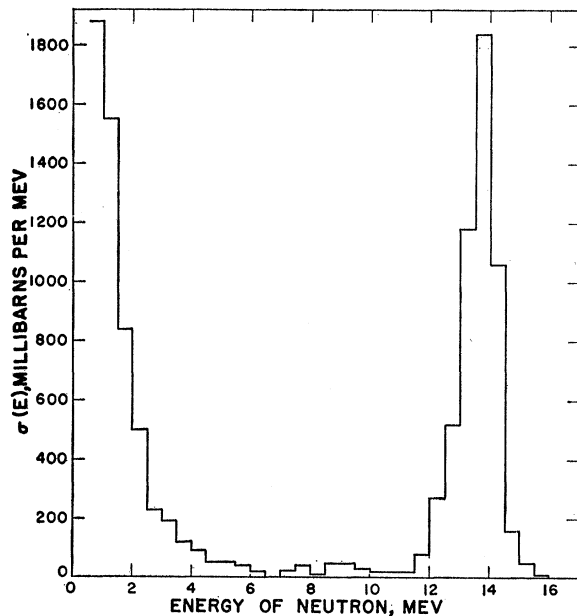


FIG. 5. Space-integrated energy distribution of the neutrons from 14-Mev neutrons on Ta.

<sup>11</sup> J. M. B. Lang and K. J. Le Couteur, Proc. Phys. Soc. (London) A67, 586 (1954).

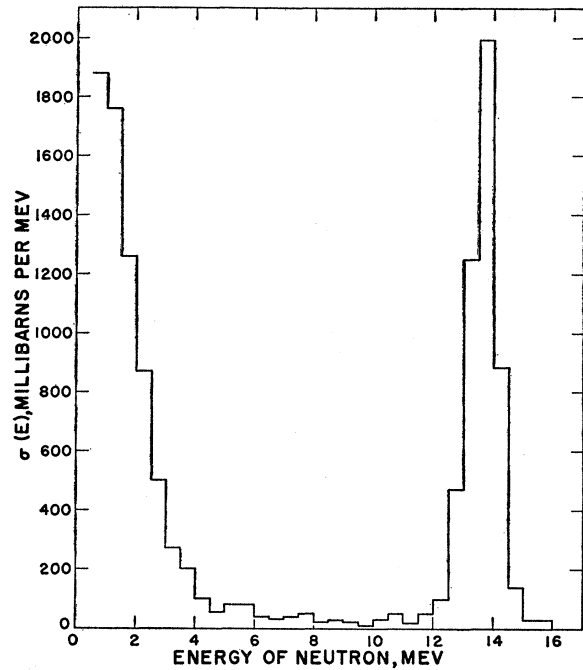


FIG. 6. Space-integrated energy distribution of the neutrons from 14-Mev neutrons on Bi.

distribution,

$$F_n(E)dE = E^{5/11}e^{-12E/11\tau_1}dE, \quad (5)$$

gives the value of  $\tau_1$  associated with the first neutron. These values were obtained by a least-squares fit weighted according to statistics.  $\tau_1$  for Bi is  $\sim 10\%$  higher than previously obtained because of the neglect of  $(n, 2n)$  effects in the previous analysis.<sup>4</sup>

On the assumption that particle emission, where energetically possible, precludes de-excitation by gamma emission, one can calculate the first-neutron distribution normalized to one-half the emission cross section from zero to  $[14 \text{ Mev} - (\text{B.E. of neutron} + 0.5 \text{ Mev})]$ .<sup>12</sup> In

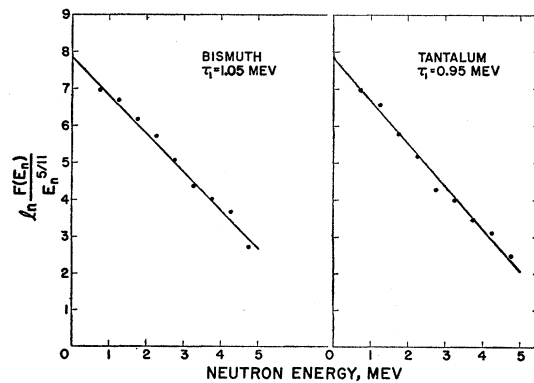


FIG. 7. Plot of  $\ln[F(E_n)/E_n^{5/11}]$  vs  $E_n$  for Ta and Bi.  $E_n$  represents the energy of the emitted neutrons.

<sup>12</sup> D. M. Van Patter and Ward Whaling, Revs. Modern Phys. 26, 402 (1954).

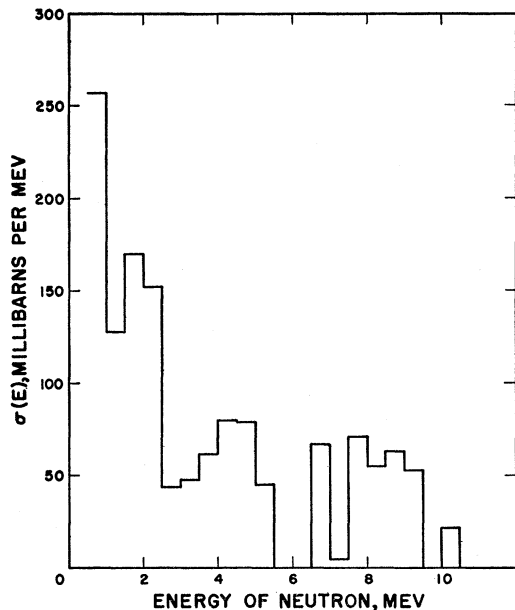


FIG. 8. Space-integrated spectrum for Be.

like manner, the  $\tau$  values associated with the evaporation of the second neutrons can be obtained by assuming the spectrum to be represented by Eq. (4) after the first-neutron contribution has been subtracted. This treatment gives a temperature of 0.4<sub>6</sub> Mev for Ta and 0.5<sub>3</sub> Mev for Bi for second-neutron emission.

Figure 8 displays the space-integrated spectrum for Be as determined by the sphere experiment. Known virtual levels at 2.4 and 7.9 Mev are in evidence but the resolution is poor due to second-neutron emission and center-of-mass motion.

If the nonelastic cross section is defined by

$$\sigma_i = \sigma_{n, n'} + \sigma_{n, 2n},$$

the cross section for the emission of nonelastic neutrons is given by

$$\sigma_e = \sigma_{n, n'} + 2\sigma_{n, 2n}.$$

The present data therefore yield values of  $\sigma_e$ ,  $\sigma_{n, n'}$ ,  $\sigma_{n, 2n}$ , and  $\sigma_i$  for Be, Ta, and Bi. These cross sections, given in Table I, depend upon the extrapolation to zero energy and upon the assumption that an  $(n, 2n)$  reaction is realized whenever the energy of the first neutron is low enough to make the emission of the second neutron energetically possible by at least 0.5 Mev.

The emission cross section should be consistent with  $\sigma_i(M-T)/(1-T)$  as determined by sphere experiments<sup>13</sup> and these measurements are also listed in Table I. The close agreement between the values in columns 6 and 7 for Bi indicates a negligible absorption cross section.

The elastic scattering angular distributions shown in Fig. 9 are valuable only insofar as they exhibit the

<sup>13</sup> E. R. Graves and R. W. Davis, Phys. Rev. **97**, 1205 (1955).

magnitude of large-angle scattering since the angular resolution ( $\pm 8^\circ$ ) is not adequate to show the diffraction minima at the forward angles.

## V. DISCUSSION

The spatial and spectral distributions displayed in Figs. 3-6 serve to identify that fraction of interactions which proceeds by direct interaction as distinguished from that which goes through a compound nucleus.

At the excitation energy of the present experiment the compound-nucleus model would seem to apply to roughly 85 to 90% of the nonelastic collisions. It is these collisions which give rise to the "Maxwellian"-type energy distribution and the spatial isotropy. These two characteristics also imply zero net interference between levels in the compound nucleus, a residual nucleus level density proportional to  $2j+1$ , and level widths independent of energy—all basic features of the statistical model. The remaining 10 to 15% of nonelastic collisions cannot be fit, even qualitatively, into the statistical model of the compound nucleus. In fact one looks to the other extreme of direct interactions to account for the forward-peaked distributions of the high-energy neutrons.

The success of the shell model and of the optical model forces one to accept the proposition that, to some extent, a nucleon can move rather freely inside a nucleus. On the other hand, many experiments have conclusively demonstrated the occurrence of resonances which can only be associated with levels in a compound nucleus and are thus indicative of strong interactions. To these two kinds of interactions one must now add direct interactions,<sup>14</sup> the products of which tend to "remember" the forward momentum of the incident particle. These reactions must be classified somewhere between the two extremes of the optical and statistical models.

Weisskopf<sup>15</sup> has recently suggested a picture of the nuclear process which unites the reaction mechanisms mentioned above and is in harmony with experimental observations. Instead of the two-stage Bohr description,

TABLE I. Cross section in barns for 14-Mev neutrons on Be, Ta, and Bi.<sup>a</sup>

Element	$\sigma_{n, n'}$	$\sigma_{n, 2n}$	This experiment $\sigma_i$	Previously reported $\sigma_i$	$\sigma_e$	Reference 13 $\sigma_i(M-T)/(1-T)$
Be	$\sim 0$	$0.42 \pm 0.07$	$0.42 \pm 0.07$	$0.37^b$	$0.84 \pm 0.14$	...
Ta	$0.17 \pm 0.03$	$1.8 \pm 0.3$	$2.0 \pm 0.4$	...	$3.8 \pm 0.5$	...
Bi	$0.17 \pm 0.03$	$2.3 \pm 0.3$	$2.4 \pm 0.4$	$2.53^c$	$4.7 \pm 0.5$	4.40

<sup>a</sup> Uncertainties listed include only those arising from neutron detection.  $\sigma_e$  refers to emission cross section extrapolated to zero energy, and  $\sigma_i$  to nonelastic cross section.

<sup>b</sup> Taylor, Lönsjö, and Bonner, Phys. Rev. **100**, 174 (1955).

<sup>c</sup> See reference 13.

<sup>14</sup> Bernardini, Booth, and Lindenbaum, Phys. Rev. **85**, 826 (1952).

<sup>15</sup> V. F. Weisskopf, Revs. Modern Phys. **29**, 174 (1957) and Physica **22**, 952 (1956); see also H. A. Bethe, Physica **22**, 941 and 947 (1956).

Weisskopf suggests dividing a nuclear reaction into three successive stages—an independent-particle stage, a compound-system stage, and a final stage. The first stage applies only to what happens in the entrance channel and can be represented by a complex square-well potential. At low neutron energies, where the exclusion principle is most effective, the absorption term which is represented by the complex part of the square-well potential is small and the reaction rarely proceeds past this stage. Under these circumstances the cloudy crystal-ball model is quite effective in predicting total cross sections and in describing the angular distribution of the reaction products, since mostly elastic scattering is involved. However, at higher energies the cross section for nonelastic processes approaches half the total cross section and so the second and third stages are important. The compound system includes, as one mode, the formation of a compound nucleus and, as another, direct interactions. The final stage encompasses the decay of the compound nucleus as well as the products of direct interactions.

Brown and Muirhead<sup>16</sup> have calculated the cross sections, as a function of angle, for the emission of neutrons by direct interactions from Bi irradiated with 14-Mev neutrons. They represent the nucleus as a Fermi gas of nucleons in which the incident particle interacts individually with the bound nucleons. The angular distribution for the emission of 4- to 12-Mev neutrons from Bi is the dotted line in Fig. 4. The agreement with our data is quite satisfactory. A Monte-Carlo calculation by Tomasini,<sup>17</sup> based on similar assumptions, indicates that direct interactions should contribute no more than 3% of the neutrons below 6 Mev, again in accord with our data.

Thus far, the only direct comparison which can be made with our data is to be found in the work of O'Neill<sup>18</sup> who, by time-of-flight measurements at two angles, concludes that the low-energy neutrons emitted when 14-Mev neutrons are incident upon Pb are isotropic. A less direct comparison is the work of Gugelot<sup>19</sup> with 18-Mev protons. Here, also, the low-energy inelastic proton spectra obtained from heavy elements are isotropic while the high-energy protons are forward peaked. The energy and angular distributions of photoneutrons from 70-Mev x-rays on heavy elements<sup>20</sup> also fall into the same pattern.

At still higher energies the preponderance of evidence<sup>21</sup> lends additional support to the interpretation

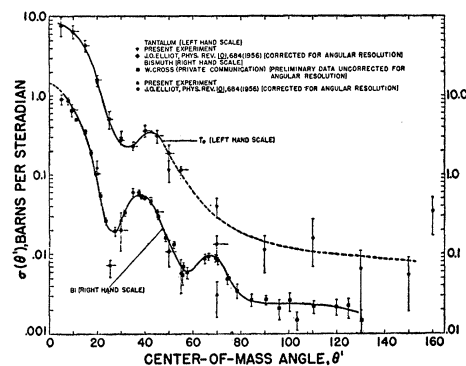


Fig. 9. Elastic scattering angular distributions for 14-Mev neutrons on Ta and Bi.

adopted for the present data. At these energies, in contradistinction to the energy of the present experiment, the direct-interaction mode does not preclude compound-nucleus formation. Corresponding to direct interaction, usually referred to as the cascade stage, high-energy particles emerge with a preference for the forward hemisphere. Following this stage occurs the evaporation of low-energy particles from the highly excited residual nucleus and these particles appear to be isotropically distributed in the center-of-mass system.

In the intermediate energy region the experiments of Eisberg *et al.*<sup>22</sup> show strongly anisotropic angular distributions of the protons resulting from nonelastic interactions of 31-Mev protons and 40-Mev alpha particles with heavy nuclei. However, here it must be emphasized that evaporation products are strongly suppressed by the Coulomb barrier and that the non-elastic cross sections observed are the same order of magnitude as the cross sections for the assumed direct interactions in  $(n,n')$  experiments at 14-Mev incident neutron energy.

The authors are indebted to the microscopy staff of Group P-10 of the Los Alamos Physics Division for the plate analysis work, and to Dr. J. H. Coon and R. W. Davis for making available the 14-Mev neutron source. It is also a pleasure to acknowledge the assistance of Dr. Glenn M. Frye in the early phases of the experiment. The authors are grateful to Dr. R. B. Leachman for constructive criticism of the manuscript.

D. M. Skyrme and W. S. C. Williams, *Phil. Mag.* **42**, 1187 (1951); J. A. Hofmann and K. Strauch, *Phys. Rev.* **90**, 449 (1953); Lock, March, and McKeague, *Proc. Roy. Soc. (London)* **A231**, 368 (1955); and L. E. Bailey, University of California Radiation Laboratory Report UCRL-3334, 1956 (unpublished).

<sup>22</sup> R. M. Eisberg, University of California Radiation Laboratory Report UCRL-2240, 1953 (unpublished); G. J. Igo, University of California Radiation Laboratory Report UCRL-2242, 1954 (unpublished); Eisberg, Igo, and Wegner, *Phys. Rev.* **100**, 1390 (1955).

<sup>16</sup> G. Brown and H. Muirhead (private communication).

<sup>17</sup> A. Tomasini, *Nuovo cimento* **12**, 134 (1954).

<sup>18</sup> G. K. O'Neill, *Phys. Rev.* **95**, 1235 (1954).

<sup>19</sup> P. C. Gugelot, *Phys. Rev.* **93**, 425 (1954).

<sup>20</sup> W. R. Dixon, *Can. J. Phys.* **33**, 785 (1955).

<sup>21</sup> Harding, Lattimore, and Perkins, *Proc. Roy. Soc. (London)* **A196**, 325 (1949); D. H. Perkins, *Phil. Mag.* **41**, 138 (1950);